# Influence of $BaZrO_3$ dopant concentration on properties of $YBa_2Cu_3O_{6+x}$ films in magnetic fields up to 30 T

H. Huhtinen,[1,a)] M. Irjala,[1,2] P. Paturi,[1] M. A. Shakhov,[1,3] and R. Laiho[1]
[1]*Department of Physics and Astronomy, Wihuri Physical Laboratory, University of Turku, FI-20014 Turku, Finland*
[2]*Graduate School of Materials Research, Turku, Finland*
[3]*A. F. Ioffe Physico-Technical Institute, St. Petersburg 194021, Russia*

(Received 22 October 2009; accepted 27 January 2010; published online 4 March 2010)

The effect of $BaZrO_3$ (BZO) dopant concentration on superconducting properties in $YBa_2Cu_3O_{6+x}$ thin films is investigated in a wide magnetic field range up to 30 T. Based on the magnetization and resistivity measurements, the optimal BZO concentration for flux pinning is found to be 4% up to 20 T and increasing up to around 8% in higher fields. This result is qualitatively explained by a model where more BZO is needed in order to organize optimal columnar defect structure at high fields because the amount of single BZO particles acting as isotropic point pinning centers is increased, especially in high BZO concentrations. This means that for applications of thin film or coated conductor structures carried out at high magnetic fields, even higher dopant concentration than used in a low-field range should be produced in order to attain the optimal flux pinning conditions. © *2010 American Institute of Physics*. [doi:10.1063/1.3329539]

## I. INTRODUCTION

The development of large-scale applications of high-temperature superconductors (HTS) such as coated conductors and thin films for the electric power industry has received a lot of technological and scientific interests, also when very high magnetic fields are generated.[1] For such applications, the requirement of optimized flux pinning needs, undoubtedly, some modifications for the artificial pinning structure that has earlier been optimized mostly at 77 K and in applied magnetic fields around 1 T. In the near future, the appreciation and implementation of this challenge is one of the most important tasks in the field of applied superconductivity.

For improving the pinning properties and increasing the critical current, the optimal way is to introduce anisotropic, nonsuperconducting columnar defects that accommodate the vortex core of diameter $\approx 2\xi$ [3 nm for $YBa_2Cu_3O_{6+x}$ (YBCO) at 0 K (Ref. 2)] along the external magnetic field over the whole thickness of the sample.[2–6] For this situation, the efficiency to prevent the motion of the magnetic flux vortices is ideal when the density of the columns is equivalent to the density of the vortex lines (matching field, $B_\Phi$). The vortex pinning problem is much more complicated in high magnetic fields when the vortex-vortex interaction becomes important, or in the case where a mixture of interplaying linear pinning defects and individual randomly distributed isotropic pinning centers occurs,[2,7–9] which is a usual situation in samples where second-phase inclusions are chemically formed into the superconductor.[10–12]

In practice, the columnar defects have been artificially introduced in HTS materials by irradiation with high-energy ions or protons,[3,13,14] but a more functional method for application point of view is to add a second-phase material by chemical doping into the superconductor lattice.[15] The most effective way to enhance flux pinning in YBCO films is to organize a network of self-assembled $BaZrO_3$ (BZO) nanodots and nanorods usually aligned along the YBCO *c*-axis.[16] The results of these kinds of doped $ReBa_2Cu_3O_{6+x}$ compounds are very promising and a large amount of different dopant materials has already been tested and optimized.[17–19] Similar types of nanodots and nanoscale columnar defects were afterwards obtained, also in other matrices such as $NdBa_2Cu_3O_{7-\delta}$ and $ErBa_2Cu_3O_{7-\delta}$.[20–22] According to the latest results, the ratio between randomly distributed nanoparticles and columnar defects, as well as their angular alignment, can be controlled by varying the growth temperature or using vicinal substrates during the deposition process.[8,9,23]

Unfortunately, the optimization of these materials are usually made within a relatively narrow temperature and magnetic field range, although it is clearly demonstrated that many interesting phenomena are expected to occur in high magnetic fields.[10,24,25] Especially, superconducting properties such as critical current density and irreversibility line (IRL) are found to have different behavior at high fields,[26,27] and therefore it is understandable that optimization of the pinning mechanism should also be made in this range.

In this work, we have systematically studied the pinning properties of YBCO thin films in a wide range of external magnetic fields up to 30 T. A way of optimization of BZO dopant concentration in YBCO lattice for high magnetic field applications is also presented.

## II. EXPERIMENTAL DETAILS

The films were prepared by pulsed laser deposition from undoped and BZO-doped YBCO targets sintered from nanocrystalline powders.[28,29] The dopant concentration is varied containing 0, 1, 2.6, 4, 5, 7.5, and 9 wt % of BZO. Details of

a)Electronic mail: hannu.huhtinen@utu.fi.

 

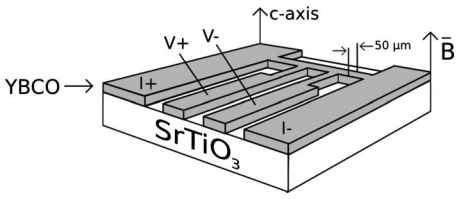


FIG. 1. A schematic drawing of the experimental setup mounted inside the solenoid in pulsed magnetic field measurements.

the preparation of nanophase targets and films are described elsewhere.[30,31] For transport measurements, the films were patterned to 50-$\mu$m-wide stripes and the thickness of the films was 150 nm as measured over the stripe edge by atomic force microscopy. The structural characterization of the films was performed using Philips X'pert Pro diffractometer with a Schultz texture goniometer.

Magnetic measurements were made with a Quantum Design Physical Property Measurement System. The superconductor critical temperatures $T_c$ were determined with ac magnetization measurements in the range of 10–100 K (ac field of 0.1 mT), and the hysteresis loops up to 8 T were obtained by dc magnetization. The critical current densities $j_c$ were determined from the Bean model for rectangular shape film: $j_c = 2\Delta m/[a(1-a/3b)V]$, where $a$ and $b(b \geq a)$ are the width and the length of the sample, $V$ is the sample volume, and $\Delta m$ is the opening of the hysteresis loop.[32–34] Transport measurements were made using a standard four-point method in a pulsed magnetic field system using 8 ms field pulse duration. During the field pulses, the resistivity of the films $\rho(B)$ was measured at temperatures 65, 70, 77, 85, and 88 K and with different transport currents up to 100 mA ($\approx$1.4 MA/cm$^2$). The measurements were limited between 65 K and the transition temperature, since already at 60 K, the irreversibility field is above 30 T and therefore over the possible measuring range. The high magnetic field transport measurements of YBCO stripe were made in the maximum Lorentz force configuration, where the measurement current $i$ was applied along the $a/b$ plane and the magnetic field $B$ parallel to the $c$-axis and perpendicular to $i$. The schematic picture of the measurement geometry is shown in Fig. 1.

## III. RESULTS

Structural properties of our undoped and BZO-doped YBCO films were published earlier.[10,28,35] X-ray diffraction showed that BZO grows epitaxially by cube-on-cube with YBCO and the texture analysis revealed that films are completely textured in the $ab$-plane except 9% BZO-doped, where 5% of the material is rotated in-plane by 45° from the $SrTiO_3$ (STO) (001) direction. In addition, all the films were $c$-axis oriented and therefore the amount of $a$-axis oriented material was less than 2% and did not depend on BZO content. The twinning of the films was investigated by measuring the $\Delta\phi$ split of the (212)/(122) peaks that was found to decrease with increasing BZO concentration. This effect is explained by the film structure where nanosized BZO particles participate in the relaxation processes of along the certain directions developed stresses and strains. The twinning and the distribution of BZO were also investigated from the

TABLE I. Temperature dependence of the pinning potential values $U(B,T)$ calculated from the fitted $U_0$ and $\alpha$ values at 15 T for the undoped (0 wt %) and BZO-doped (1–9 wt %) YBCO films.

| Sample (%) | $T_c$ (K) | $U$ (15 T, 65 K) (K) | $U$ (15 T, 77 K) (K) | $U$ (15 T, 88 K) (K) |
|---|---|---|---|---|
| 0 | 90 | 561 | 30 | 1 |
| 1 | 90 | 913 | 73 | 2 |
| 2.6 | 90 | 1104 | 73 | 3 |
| 4 | 88 | 756 | 48 | 3 |
| 5 | 88 | 913 | 73 | 7 |
| 7.5 | 87.5 | 938 | 73 | 7 |
| 9 | 86.5 | 1532 | 126 | ⋯ |

planar view and cross-section transmission electron microscopy (TEM) images.[35] Irregularly shaped twin domains and curved twin planes together with relatively small growth islands lead to a network of correlated pinning sites even in undoped YBCO films deposited from a target that was sintered from nanopowder. The TEM images of 3.9% BZO-doped YBCO films reveal film penetrating and $c$-axis aligned network of columnar nanorods of diameter 5–10 nm, having spacings of 15–20 nm. The calculated volumes of the BZO columns show that nanorods are roughly half occupied by BZO with distorted YBCO in between.[10] In the planar view TEM images, the number of BZO particles is found to increase with doping while the size of particles remains the same. In addition, the YBCO lattice is well-aligned in the regions more than 5 nm away from the BZO particles, whereas in the vicinity of BZO, several edge dislocations were observed.[35] The average areal densities of the BZO particles were also calculated from planar view images where the columns form approximately an equilateral triangular lattice. The areal densities of BZO are 1300, 2500, and 4200 $\mu$m$^{-2}$ for the films doped with 2.9, 3.9, and 9.0 wt % of BZO, respectively, and therefore the actual dependence is not linear.[28]

Temperature dependences of the real part of ac magnetization show that the onset $T_c$ is slightly decreased with increasing BZO content, being 86.5 K for 9% BZO-doped YBCO (Table I). The shapes of the $j_c(B)$ curves for undoped and BZO-doped YBCO films measured from the hysteresis loops at 10 K in Fig. 2 are completely different. The shape of the $j_c(B)$ curve of undoped YBCO is much steeper, giving

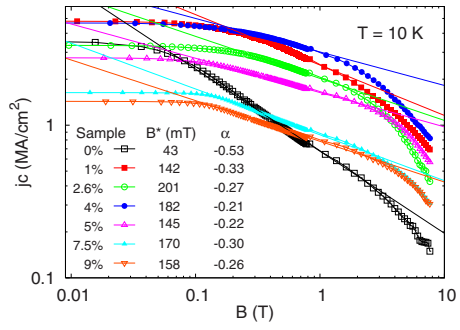


FIG. 2. (Color online) Magnetic field dependence of $j_c$ determined from the hysteresis loops at 10 K. The lines are the fits to Eq. (1). The inset table shows the accommodation field values $B^*$ and the power-law exponents $\alpha$ in fits to Eq. (1).

the smallest $j_c$ above $B=600$ mT. This is in line with the accommodation field values $B^*$, which are determined by the criterion $j_c(B^*)/j_c(0)=0.9$.[36] The inset table of Fig. 2 shows that $B^*$ is clearly the smallest for undoped YBCO and has a maximum value between 2.6% and 4%, which is close to the earlier magnetically observed optimal concentration.[28] The doping increases unambiguously the critical current density in a higher magnetic field range above 100 mT and the highest value of $j_c$ is obtained for 4% BZO-doped film as observed also earlier.[28] The shapes of the $j_c(B)$ curves are also compared by using a double logarithmic plot described by the equation

$$j_c(T,B) = A(T)B^{\alpha}, \tag{1}$$

limited to the values of $B > B^*$ above the low-field plateau of $j_c(B)$ and the high-field limit where the crossover between the relatively strong pinning region and the steeper decrease due to flux creep is observed. The power-law exponents $\alpha$ are shown also in the inset of Fig. 2, and it can be concluded that $\alpha=-0.53$ for undoped YBCO is in agreement with the theories,[37–39] where $\alpha=-0.5$ and $-5/8$ are connected to a low density of strong pinning centers at relatively low fields. The exponent values $\alpha \approx -0.3$, which is the case for 1%–2.6% and again for 7.5%–9% BZO-doped YBCO films, are usually associated with strong vortex pinning, where $j_c$ is less field dependent.[40] Even the smaller value of $\alpha \approx 0.2$ is observed for our films doped with 4%–5% of BZO. These results fit perfectly with our structural analysis discussed above and also with the model where twin boundaries, dislocations, and BZO nanorods are altogether responsible for the enhanced $j_c$ values and the shape of the $j_c(B)$ curves, too.[8,41]

Temperature dependences of $\rho(B)$ measured at the probe current of 1 mA ($\approx 1.5\times 10^4$ A/cm$^2$) are shown in Figs. 3(a)–3(g). From these curves, it can be clearly seen that in comparison with undoped YBCO films, the average rise of the resistivity starts in higher magnetic fields in BZO-doped YBCO films and the effect is more pronounced at temperatures below 77 K. The dependence of the resistivity on temperature and magnetic field can be expressed by a function $\rho(T,B) \propto e^{-U(B)/T}$, where $U(B)=U_0/B^{\alpha}$ is the power-law field dependent pinning potential.[42] Therefore at constant temperature and in our measurement geometry, the behavior of $\rho(B)$ can be given in the form

$$\rho(B) = \rho_0 e^{-U_0/TB^{\alpha}}, \tag{2}$$

where $\rho_0$ is the normal state resistivity. Figures 3(a)–3(g) show also the fits of the experimental data of $\rho(B)$ at different temperatures with Eq. (2) using $\rho_0$, $U_0$, and $\alpha$ as fitting parameters. The values of fitted pinning energies, listed in Table I, show that generally, BZO doping also increases $U(B)$ in the temperature range below the transition temperature. The calculated pinning energies at 65 K for undoped YBCO are in line with earlier estimated $U$ values from 0.05 to 0.2 eV (Ref. 43 and 44), and $U(B)$ values for doped films are in good agreement with the results, where $BaSnO_3$ and BZO doping[44] have been observed to globally increase the pinning force within the same temperature range than in our experiments.

The irreversibility fields $B_{irr}$ were determined from the $\rho(B)$ curves at the point where the resistivity exceeds the noise level of $\approx 3\times 10^{-7}$ Ω cm. As can be seen from the temperature dependences of the irreversibility fields (Fig. 4), the IRL, which indicates the solid-liquid phase transition of the vortex matter, is located more than 5 T higher fields for the 9% BZO-doped YBCO film at $T/T_c < 0.9$ than in the undoped film. The IRL curves of other BZO concentrations are situated in between the curves of 0% and 9% BZO-doped YBCO films. At temperatures close to the transition temperatures, the relatively low BZO dopings seem to be more effective having IRL above the curve of 9% BZO concentration. These results are in line with our earlier measurements, where the difference between the IRL of undoped and BZO-doped nanostructured YBCO films is relatively small, especially when compared to the IRL of films deposited from micrograined YBCO targets.[10] It is also good to notice that the BZO concentration is not the only thing that matters since the superconducting properties strongly depend on the type and the density of the defects, and therefore isotropic pinning centers, and on the other hand columnar defects have different types of effect for, e.g., IRL.[12,45]

The magnetic field dependences of $j_c$ at 65 K determined from the pulsed magnetic measurements are shown in Fig. 5. As can be seen from this graph, where $j_c(B)$ is shown at 65 K, all the BZO-doped YBCO films can carry relatively high critical current densities over $10^5$ A/cm$^2$ in fields of 20 T, whereas the undoped YBCO has clearly the smallest $j_c$ level in this high magnetic field range. BZO concentration dependence is not so straightforward but it can be concluded that according to the transport measurements, higher BZO contents are more effective when compared to the $j_c$ values obtained from magnetic measurements. For example, in Fig. 5, the 9% BZO-doped YBCO has the highest $j_c$ in fields above 23 T, whereas the same concentration film had the smallest magnetically measured $j_c$ in fields below 600 mT, as obtained from Fig. 2. In principle, there is a relatively good agreement between magnetic and transport measurements, and $j_c$ is obtained with good accuracy, especially in thin films with applied field parallel to the short dimension of the sample.[46] Therefore, we can conclude that the difference between low-field and high-field measurements originates from the field dependence of the BZO concentration.

## IV. DISCUSSION

For making an optimization of BZO concentration $n$ with magnetic field, using $j_c$ data of magnetic measurements below 8 T at 10 K (Fig. 2) and on the other hand using resistivity results obtained at 65 K in higher magnetic field range above 15 T (Fig. 5), we have made a cross-section of the experimental $j_c$ data with fixed magnetic field $B$ values. The BZO concentration that gives the maximum $j_c$ in the certain field $n_{opt}$ is calculated from the parabolic fit to $j_c(n)$ that gives an approximation of the data trend (inset of Fig. 6). The error bars in $n_{opt}$ data are also estimated from the fits. In the lower magnetic field range (on the left side of the Fig. 6), $n_{opt}$ increases almost exponentially near zero field and then saturates up to the level of 4% of BZO. This is in

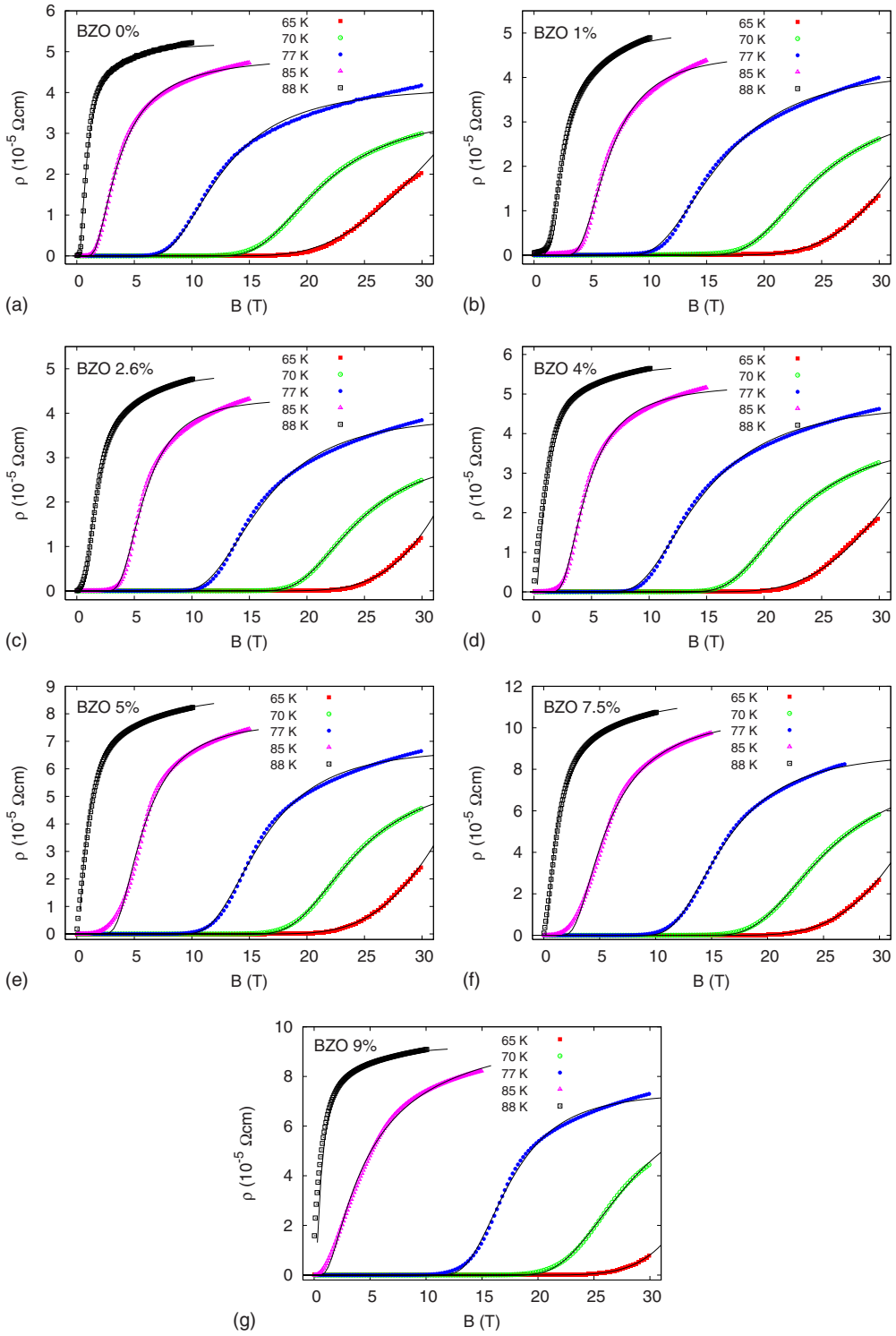


FIG. 3. (Color online) Magnetic field dependence of the resistivity $\rho(B)$, measured at different temperatures for (a) undoped and the [(b)–(g)] 1, 2.6, 4, 5, 7.5, and 9 wt % BZO-doped YBCO films, respectively. The lines are fits to Eq. (2).

agreement with the results where the optimization was made using the irreversibility temperature in the thermally activated flux-flow (TAFF) regime.[12] However, the $n_{opt}$ curve found in this work lies roughly 1 wt % higher than in measurements made in the TAFF regime. This can be explained by the temperature range difference where a smaller dopant concentration is observed to be more effective at high temperatures.[47,48] Also, the increase in the coherence length $\xi$ with temperature leads to a wider vortex core[2] and therefore the optimization of BZO content near $T_c$ gives lower $n_{opt}$. Temperature dependence of $\xi=\xi_0(1-T/T_c)^{-1/2}$ means that the coherence length does not change remarkably between 10 and 65 K, but a significant increase takes place near $T_c$, and therefore comparison with the results optimized in the TAFF region is not optimal.[12] If the diameter of the columnar defect increases with BZO additions, as predicted in Ref. 11, the vortex pinning should be more effective at high temperatures where the size of the vortices was increased. Because

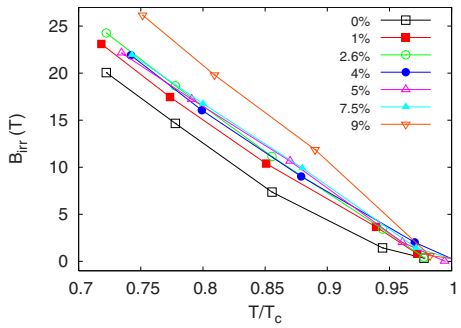


FIG. 4. (Color online) Temperature dependence of $B_{irr}$ for YBCO films doped with different BZO concentrations. The lines are to guide the eye.

the pinning properties that lead to a different shape of the $j_c(B)$ curve depend mostly on $\xi(T)$, we can with good reason compare the values of $n_{opt}$ in the two different field ranges shown in Fig. 6.

When looking at the tendency in the high magnetic field range, the $n_{opt}$ value is almost a constant up to 20 T but the shape of the $j_c(n)$ curve starts to change (see inset of Fig. 6) since another shoulder starts to appear in the BZO concentration dependent $j_c$ curve at higher magnetic fields above 20 T. This leads to a steeper increase in average $n_{opt}$ up to BZO content of 7.5% as can be seen in Fig. 6. A similar type of effect has also been observed earlier in the lower field range below 5 T, where the low-field plateau of $j_c(B)$ is lengthened and the accommodation field $B^*$ is increased in YBCO films doped with BZO.[29] In addition, already at 3 T, the 6 mol % of BZO in YBCO film was obtained to have the strongest flux pinning effect at temperatures below 30 K, while in the self-field and at 77 K, the BZO content of 1%–4% gives usually the highest $j_c$.[11,47] For undoped bulk YBCO, a crossover between power-law and almost linear dependent IRL $H_{irr}(T)$ is also found to be around 20 T,[26] which is the same value we have as a limiting value in our $n_{opt}$ curve of Fig. 6. From our results shown above, we can easily get two different regimes for optimal BZO concentration $n_{opt}$, indicating that the pinning efficiency of the BZO particles depends on temperature and the magnetic field.

The matching field $B_\Phi$, calculated from the size and the distribution of the columnar defects in 4% BZO-doped films, is around 5 T that fits perfectly to the middle point of the low-field range data on the left panel of the Fig. 6. At higher fields the situation is not so straightforward, but qualitatively

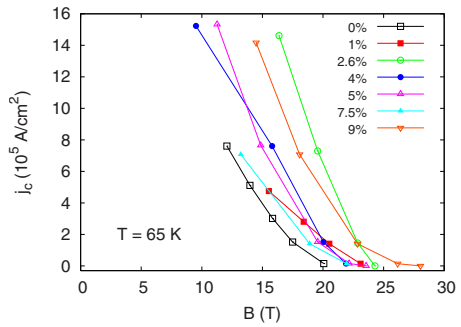


FIG. 5. (Color online) The field dependences of the critical current densities of the undoped and BZO-doped YBCO films at 65 K determined from the pulsed magnetic field data.

the increase in $n_{opt}$ can be understood by an increased amount of isotropic pinning centers in the lattice that do not form linear defects until the amount of BZO is high enough. As discussed above, the density of the columnar defects does not increase linearly with doping concentration, and therefore even higher $n_{opt}$ is needed for producing enough pinning sites for optimal flux pinning properties in the high magnetic field range. In addition, deposition parameters including strain and dislocation alignments are suggested to play a significant role in forming columnar defects,[9] e.g., lower deposition temperature produces a combination of dopant nanoparticles and nanorods, and on the other hand, the length of the columns became shorter when the growth temperature was decreased.[8] Besides, an inverse correlation between $c$-axis peak height in angular dependent critical current $j_c(\theta)$ measurements and exponent $\alpha$ [Eq. (1)] is observed.[8] Since, in our case, $\alpha$ starts to increase above 5% of BZO, pure columnar and $c$-axis oriented pinning structure is not any more obvious. This clearly supports the theory where single particles are formed together with BZO columnar nanorods above BZO concentration of 5%. Moreover, a renormalized anisotropic parameter $\gamma=1/\epsilon=5-7$ in scaling relation indicates pointlike random pinning,[49] which is not the case in our 4% BZO-doped YBCO films, where $\gamma_{eff}\approx 1.5$.[50] For the increased amount of BZO above 4%, the $c$-axis peak in $j_c(\theta)$ decreases which could lead to a larger $\gamma_{eff}$.[11] This again supports our model where the combination of different types of defects are responsible for pinning in higher dopant concentrations. However, the behavior of $n_{opt}$ shows certainly that in high-field applications near liquid nitrogen temperature, the BZO content in YBCO matrix should be higher than in devices realized at low temperatures and low fields.

## V. CONCLUSIONS

We have systematically investigated the influence of BZO dopant concentration on superconducting properties in nanostructured YBCO thin films by measuring the magnetization and resistivity in wide magnetic field and temperature ranges. Low-field measurements show that BZO doping increases the accommodation field and the value of $j_c$ in a way that the optimal BZO concentration is around 4%. However,

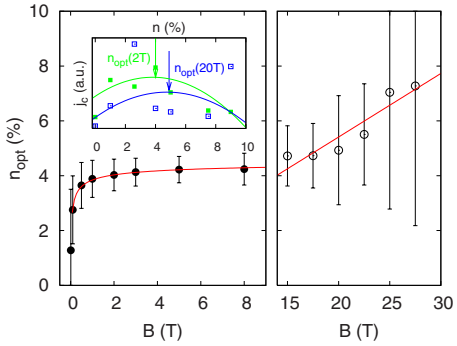


FIG. 6. (Color online) Magnetic field dependence of optimal BZO concentration $n_{opt}$ measured in two different field ranges. The error bars are calculated from the parabolic fits to the experimental BZO concentration dependent $j_c$ data, measured at different magnetic fields. The lines in the main panels are fits to exponential increase at low fields on the left and to the linear behavior on the right.

strongly doped YBCO films (7.5%–9%) become relatively more effective in the fields above 1 T, where $j_c(B)$ decreases slower than in samples with smaller BZO concentrations, but still they cannot reach the $j_c$ values of 4% BZO-doped films. On the other hand, transport measurements in high fields up to 30 T indicate that the obtained $\rho(B)$ is shifted to higher fields when films were doped with BZO. In addition, the pinning potential and irreversibility field were increased in whole measured temperature range for BZO-doped YBCO films. In contrast with the low-field results, the optimization of BZO concentration from the magnetic field dependences of $j_c$ data suggests that in fields above 20 T an optimal BZO content increases even more, almost up to 8%. This steeper growth of the optimal BZO content is explained by the model where isotropic pinning sites are formed in addition to nanorods at BZO concentrations above 4%. More complete columnar pinning centers are achieved again at about 8% of BZO. Generally, this paper shows the possibility to use even higher BZO concentrations in YBCO matrix in order to achieve more effective pinning structure for future applications carried out at high magnetic fields.

## ACKNOWLEDGMENTS

The Wihuri Foundation and the Academy of Finland are acknowledged for financial support.

[1]D. Larbalestier, A. Gurevich, D. M. Feldmann, and A. Polyanskii, Nature (London) **414**, 368 (2001).
[2]G. Blatter, M. Feigel'man, V. Geshkenbein, A. Larkin, and V. Vinokur, Rev. Mod. Phys. **66**, 1125 (1994).
[3]L. Civale, A. D. Marwick, T. K. Worthington, M. A. Kirk, J. R. Thompson, L. Krusin-Elbaum, Y. Sun, J. R. Clem, and F. Holtzberg, Phys. Rev. Lett. **67**, 648 (1991).
[4]L. Civale, Supercond. Sci. Technol. **10**, A11 (1997).
[5]A. V. Samoilov, M. V. Feigel'man, M. Konczykowski, and F. Holtzberg, Phys. Rev. Lett. **76**, 2798 (1996).
[6]B. Dam, J. M. Huijbregtse, F. C. Klaassen, R. C. F. van der Geest, G. Doornbos, J. H. Rector, A. M. Testa, S. Freisem, J. C. Martinez, B. Stuble-Pumpin, and R. Griessen, Nature (London) **399**, 439 (1999).
[7]A. Polkovnikov, Y. Kafri, and D. R. Nelson, Phys. Rev. B **71**, 014511 (2005).
[8]B. Maiorov, S. A. Baily, H. Zhou, O. Ugurlu, J. A. Kennison, P. C. Dowden, T. G. Holesinger, S. R. Foltyn, and L. Civale, Nature Mater. **8**, 398 (2009).
[9]F. J. Baca, P. N. Barnes, R. L. S. Emergo, T. J. Haugan, J. N. Reichart, and J. Z. Wu, Appl. Phys. Lett. **94**, 102512 (2009).
[10]M. Peurla, H. Huhtinen, M. A. Shakhov, K. Traito, Y. P. Stepanov, M. Safonchik, P. Paturi, Y. Y. Tse, R. Palai, and R. Laiho, Phys. Rev. B **75**, 184524 (2007).
[11]S. Kang, A. Goyal, J. Li, P. Martin, A. Ijaduola, J. R. Thompson, and M. Paranthaman, Physica C **457**, 41 (2007).
[12]M. Safonchik, K. Traito, S. Tuominen, P. Paturi, H. Huhtinen, and R. Laiho, Supercond. Sci. Technol. **22**, 065006 (2009).
[13]M. Konczykowski, F. Rullier-Albenque, E. R. Yacoby, A. Shaulov, Y. Yeshurun, and P. Lejay, Phys. Rev. B **44**, 7167 (1991).
[14]L. Krusin-Elbaum, J. R. Thompson, R. Wheeler, A. D. Marwick, C. Li, S. Patel, D. T. Shaw, P. Lisowski, and J. Ullmann, Appl. Phys. Lett. **64**, 3331 (1994).
[15]T. Haugan, P. N. Barnes, R. Wheeler, F. Meisenkothen, and M. Sumption, Nature (London) **430**, 867 (2004).
[16]A. Goyal, S. Kang, K. J. Leonard, P. M. Martin, A. A. Gapud, M. Varela, M. Paranthaman, A. O. Ijadoula, E. D. Specht, J. R. Thompson, D. K. Christen, S. J. Pennycook, and F. A. List, Supercond. Sci. Technol. **18**, 1533 (2005).
[17]J. L. MacManus-Driscoll, S. R. Foltyn, Q. X. Jia, H. Wang, A. Serquis, L. Civale, B. Maiorov, M. E. Hawley, M. P. Maley, and D. E. Peterson, Nature Mater. **3**, 439 (2004).
[18]C. V. Varanasi, P. N. Barnes, J. Burke, L. Brunke, I. Maartense, T. J. Haugan, E. A. Stinzianni, K. A. Dunn, and P. Haldar, Supercond. Sci. Technol. **19**, L37 (2006).
[19]T. Kato, H. Sasaki, Y. Gotoh, Y. Sasaki, T. Hirayama, K. Takahashi, M. Konishi, H. Kobayashi, A. Ibi, T. Muroga, S. Miyata, T. Watanabe, Y. Yamada, T. Izumi, and Y. Shiohara, Physica C **445–448**, 628 (2006).
[20]S. H. Wee, A. Goyal, J. Li, Y. L. Zuev, S. Cook, and L. Heatherly, Supercond. Sci. Technol. **20**, 789 (2007).
[21]S. H. Wee, A. Goyal, J. Li, Y. L. Zuev, and S. Cook, J. Appl. Phys. **102**, 063906 (2007).
[22]R. Teranishi, S. Yasunaga, H. Kai, K. Yamada, M. Mukaida, N. Mori, T. Fujiyoshi, A. Ichinose, S. Horii, K. Matsumoto, Y. Yoshida, R. Kita, and S. Awaji, Physica C **468**, 1522 (2008).
[23]Y. Zhang, E. D. Specht, C. Cantoni, D. K. Christen, J. R. Thompson, J. W. Sinclair, A. Goyal, Y. L. Zuev, T. Aytug, M. P. Paranthaman, Y. Chen, and V. Selvamanickam, Physica C **469**, 2044 (2009).
[24]H. Nakagawa, T. Takamasu, N. Miura, and Y. Enomoto, Physica B **246–247**, 429 (1998).
[25]J. L. O'Brien, H. Nakagawa, A. S. Dzurak, R. G. Clark, B. E. Kane, N. E. Lumpkin, R. P. Starrett, N. Muira, E. E. Mitchell, J. D. Goettee, D. G. Rickel, and J. S. Brooks, Phys. Rev. B **61**, 1584 (2000).
[26]Y. Skourski, G. Fuchs, P. Kerschl, N. Kozlova, D. Eckert, K. Nenkov, and K.-H. Müller, Physica B **346–347**, 325 (2004).
[27]T. Matsushita, H. Wada, T. Kiss, M. Inoue, Y. Iijima, K. Kakimoto, T. Saitoh, and Y. Shiohara, Physica C **378–381**, 1102 (2002).
[28]M. Peurla, P. Paturi, Y. P. Stepanov, H. Huhtinen, Y. Y. Tse, A. C. Bódi, J. Raittila, and R. Laiho, Supercond. Sci. Technol. **19**, 767 (2006).
[29]K. Traito, M. Peurla, H. Huhtinen, Y. P. Stepanov, M. Safonchik, Y. Y. Tse, P. Paturi, and R. Laiho, Phys. Rev. B **73**, 224522 (2006).
[30]J. Raittila, H. Huhtinen, P. Paturi, and Y. P. Stepanov, Physica C **371**, 90 (2002).
[31]H. Huhtinen, J. Järvinen, R. Laiho, P. Paturi, and J. Raittila, J. Appl. Phys. **90**, 1521 (2001).
[32]C. P. Bean, Phys. Rev. Lett. **8**, 250 (1962).
[33]C. P. Bean, Rev. Mod. Phys. **36**, 31 (1964).
[34]H. P. Wiesinger, F. M. Sauerzopf, and H. W. Weber, Physica C **203**, 121 (1992).
[35]M. Peurla, H. Huhtinen, Y. Y. Tse, J. Raittila, and P. Paturi, IEEE Trans. Appl. Supercond. **17**, 3608 (2007).
[36]C. Cai, B. Holzapfel, J. Hänisch, L. Fernandez, and L. Schultz, Phys. Rev. B **69**, 104531 (2004).
[37]C. J. van der Beek, M. Konczykowski, A. Abal'oshev, I. Abal'osheva, P. Gierlowski, S. J. Lewandowski, M. V. Indenbom, and S. Barbanera, Phys. Rev. B **66**, 024523 (2002).
[38]G. Blatter, V. B. Geshkenbein, and J. A. G. Koopmann, Phys. Rev. Lett. **92**, 067009 (2004).
[39]F. C. Klaassen, G. Doornbos, J. M. Huijbregtse, R. C. F. van der Geest, B. Dam, and R. Griessen, Phys. Rev. B **64**, 184523 (2001).
[40]A. A. Gapud, D. Kumar, S. K. Viswanathan, C. Cantoni, M. Varela, J. Abiade, S. J. Pennycook, and D. K. Christen, Supercond. Sci. Technol. **18**, 1502 (2005).
[41]P. Paturi, M. Irjala, H. Huhtinen, and A. B. Abrahamsen, J. Appl. Phys. **105**, 023904 (2009).
[42]Y. Z. Zhang, Z. Wang, X. F. Lu, H. H. Wen, J. F. de Marneffe, R. Deltour, A. G. M. Jansen, and P. Wyder, Phys. Rev. B **71**, 052502 (2005).
[43]T. L. Hylton and M. R. Beasley, Phys. Rev. B **41**, 11669 (1990).
[44]P. Mele, K. Matsumoto, T. Horide, A. Ichinose, M. Mukaida, Y. Yoshida, S. Horii, and R. Kita, Supercond. Sci. Technol. **21**, 032002 (2008).
[45]A. I. Larkin and V. M. Vinokur, Phys. Rev. Lett. **75**, 4666 (1995).
[46]A. Sanchez and C. Navau, Supercond. Sci. Technol. **14**, 444 (2001).
[47]K. J. Song, R. K. Ko, Y. S. Lee, J. S. Yang, Y. M. Park, M. Dixit, H. S. Kim, H. S. Ha, D. W. Ha, S. Oh, D. J. Kim, C. Park, and S.-I. Yoo, Physica C **445–448**, 656 (2006).
[48]H. Huhtinen, M. Peurla, M. A. Shakhov, Y. P. Stepanov, P. Paturi, J. Raittila, R. Palai, and R. Laiho, IEEE Trans. Appl. Supercond. **17**, 3620 (2007).
[49]G. Blatter, V. B. Geshkenbein, and A. I. Larkin, Phys. Rev. Lett. **68**, 875 (1992).
[50]P. Paturi, M. Irjala, and H. Huhtinen, J. Appl. Phys. **103**, 123907 (2008).